IOP Conf. Series: Journal of Physics: Conf. Series **1489** (2020) 012015 doi:10.1088/1742-6596/1489/1/012015

Nonlinear Dynamics of a Magnetically Supported Flexible Rotor in Auxiliary Bearings

Jawaid I Inayat-Hussain

College of Graduate Studies, Universiti Tenaga Nasional, Jalan IKRAM-UNITEN, 43000 Kajang, Selangor, Malaysia

Abstract. The results of a numerical simulation on the nonlinear dynamics of a flexible rotor mounted on magnetic and auxiliary bearings are presented in this work. The focus of this work was to investigate the effect of shaft flexibility on the rotor response during load sharing operation between the magnetic and auxiliary bearings. For the range of parameters considered herein, results from the numerical simulation showed that the stiffness ratio, which represented the contact stiffness of the auxiliary bearing, was a more effective parameter, as compared to the Coulomb sliding friction coefficient, for the suppression of sub-synchronous and non-synchronous vibrations in the rotor's response. Sub-synchronous vibrations of period-2, period-4, period-8 and period-16 were observed in the response of the rotor. Non-synchronous vibration which was also seen in the rotor's response was determined to be chaos. For the case of the rotor response with variation of the stiffness ratio, the route to chaos was found to be due to a sequence of period-doubling bifurcations, where the synchronous or period-1 response bifurcated into period-2, period-4, period-8 and period-16 responses, culminating into chaotic vibration. Vibrations which are of sub-synchronous and non-synchronous nature are best avoided in the rotor's response during operation, whereby the load is shared between magnetic and auxiliary bearings, as they produce stress reversals. Such stresses can potentially cause fatigue failure of the rotors and their associated structures.

1. Introduction

Magnetic bearings, which are nonlinear in nature, have in the past found many application in rotating machinery. The main sources of nonlinearity in these bearings are due to the relationship between the magnetic bearing force with the stator-to-rotor air gap and coil current, and the cross-coupled magnetic bearing forces in the orthogonal directions [1-2]. Ji *et al*. [3] had, in the recent past, presented a considerably extensive review on the nonlinear dynamics of magnetic bearings. There has also been many articles published on the nonlinear vibrations of magnetic bearing system in the past, and some of the pertinent ones include references [4-9]. The effects of auxiliary bearings on the nonlinear response of rotating machinery supported by magnetic bearings have not been considered in most of these works. Auxiliary bearings, or also known as retainer or catcher bearings, are important machine elements in the design and operation of rotating machinery supported by active magnetic bearings. These bearings have two important functions. First, they give support to the rotating machinery while it is stationary. Second, they act as back-up bearings to protect the magnetic bearings in the event of power loss during operation. The auxiliary bearings are usually designed to have their clearances to be half of the clearances of magnetic bearings. As a consequence, there is always a possibility of contact to occur during machinery's operation. In such cases, the rotor load is shared by both the magnetic bearing and the auxiliary bearing, and this further affects the rotor-bearing system's

dynamics. Some of the important works in the past that are concerned with the dynamics of rotating machinery supported by active magnetic bearings and auxiliary bearings are briefly reviewed herein.

Past works on rotors supported by magnetic and auxiliary bearings can be conveniently categorized into two specific areas. The first is concerned with rotor drop on auxiliary bearings, which is a transient phenomenon, and the second is the load sharing between the magnetic bearing and auxiliary bearing, which is a steady-state phenomenon. Fumagalli and Schweitzer [10] showed the possibility of backward whirl with large amplitude to occur during rotor drop on auxiliary bearing. Ishii and Kirk [11] revealed that a range of support damping which are optimal exists that prevents backward whirl from occurring during rotor drop on auxiliary bearing. Kirk [12] proposed a theoretical method to determine the response of a rotor drop onto auxiliary bearing, and further validated this method during shop testing of a full scale eight stage centrifugal compressor. In the numerical work of Karkkainen *et al*. [13], it was shown that the utilization of different models to represent friction during rotor drop, and the magnitude of auxiliary bearing's clearance had almost negligible effect on the response of the rotor. Numerical and experimental works of Zeng [14] on rotor drop onto auxiliary bearings, with different support configurations, of a magnetically suspended flexible rotor revealed that the magnetic force which decays in the event of a magnetic bearing failure had insignificant influence on the rotor's response.

Past works on magnetic and auxiliary bearing load sharing had shown the occurrences of various nonlinear phenomena in the rotor's response. The work of Lawen and Flowers [15] showed that the response of the rotor was heavily dependent on the parameters of the auxiliary bearings and their respective bearing housings. Wang and Noah [16] showed the occurrences of sub-synchronous, quasi-periodic and chaotic vibrations in the response of a rotor in auxiliary bearings. In this work, however, the magnetic bearing forces were omitted in the model of the rotor-bearing system. This work indicated that the contact between the rotor and auxiliary bearing was highly nonlinear albeit the absence of the magnetic bearing forces. The response of a jet engine rotor supported by auxiliary bearings, investigated by Xie *et al*. [17], showed the occurrences of multiple solutions, sub-synchronous vibration and chaos in the rotor's response. Effects of various parameters on the rotor's response were examined in his work. The authors concluded that auxiliary bearings designed to have high support damping, low support stiffness and small clearance gave the most favorable rotor response. The response of a magnetically supported rotor in load sharing mode with auxiliary bearing, presented by Jang and Chen [18], showed various nonlinear phenomena including sub-synchronous, quasi-periodic and chaotic vibrations. Work by Zeng [19] on the response of a Jeffcott rotor on auxiliary bearings showed the existence of various regions of nonlinear phenomena over a range of rotor speed. These regions of nonlinear phenomena was found to be significantly affected by the rotor imbalance magnitude. The author then showed that the selection of appropriate damping and stiffness coefficients of the auxiliary bearing can potentially reduce the rotor whirl amplitude response. Inayat-Hussain [20-21] had presented results on the numerical simulation of a magnetically supported rigid rotor in auxiliary bearings. The work in [20] showed that, for relatively small rotor imbalance magnitudes, nonlinear vibrations in the response of the rotor could have not been identified if the auxiliary bearing forces were neglected in the rotor-bearing system model. It was further shown that non-synchronous response was dominant for the case of large rotor imbalance magnitudes, and that the variation of stiffness and Coulomb sliding friction coefficient of the auxiliary bearings had almost negligible effect on the rotor's response [21]. For relatively smaller rotor imbalance magnitudes, however, the variation of stiffness and Coulomb sliding friction coefficient were found to be effective to reduce the speed region where the non-synchronous vibration response occurred.

The present work extends the work reported in [20-21], where a flexible rotor is considered, in contrast with the work presented in [20-21] that dealt with rigid rotor. The effects of the auxiliary bearing contact stiffness and the Coulomb sliding friction coefficient on the rotor's response are examined in the work presented herein.

2. Governing Equations of the Rotor-Bearing System

In this work the rotor-bearing system is represented by a simple flexible rotor, Figure 1. The rotor has a disk of mass $2m_D$ located at its mid-span, and journal mass m_J located at each of its two bearing stations. The following assumptions were made in the formulation of the governing equations of the rotor-bearing system: (i) rotor is axially and radially symmetric, (ii) viscous damping acts on the disk located at the rotor's mid-span, (iii) location of rotor imbalance is on the disk at the rotor's mid-span, and (iv) gyroscopic effect is not considered. Due to the symmetry of the flexible rotor, it was sufficient to consider only one-half of the rotor-bearing system in the formulation of the governing equations. Displacements $\bar{x}_D$ and $\bar{y}_D$ of the geometric centre of the disk at the rotor mid-span, and displacements $\bar{x}_J$ and $\bar{y}_J$ of the geometric centre of the journal represent the motion of the rotor-bearing system. In the formulation of the equations of motion, the following forces that acts on the disk at the rotor mid-span and the bearing journal are accounted for: (i) force due to shaft elasticity, (ii) imbalance force of the rotor, (iii) viscous damping force, (iv) force due to gravity, (v) magnetic bearing force, and (vi) auxiliary bearing force. Eq. (1) presents the governing equations of the rotor-bearing system. In these equations, half-stiffness of the shaft is denoted by k_R, half-damping coefficient of the disk at the rotor mid-span is denoted by c_R, eccentricity of the rotor centre of mass is denoted by u, rotor angular speed is denoted by ω, and the gravity constant is denoted by g. The resultant magnetic bearing forces are denoted by $\bar{F}_X$ and $\bar{F}_Y$, respectively in the X and Y-directions. $\bar{F}_{AX}$ and $\bar{F}_{AY}$ are respectively the contact forces of the auxiliary bearing in the X and Y-directions.

$$
\begin{aligned}
m_D\ddot{\bar{x}}_D &= -c_R\dot{\bar{x}}_D - k_R(\bar{x}_D - \bar{x}_J) + m_D u\omega^2\cos\omega t \\
m_D\ddot{\bar{y}}_D &= -c_R\dot{\bar{y}}_D - k_R(\bar{y}_D - \bar{y}_J) - m_D g + m_D u\omega^2\sin\omega t \\
m_J\ddot{\bar{x}}_J &= \bar{F}_X + \bar{F}_{AX} - k_R(\bar{x}_J - \bar{x}_D) \\
m_J\ddot{\bar{y}}_J &= \bar{F}_Y + \bar{F}_{AY} - k_R(\bar{y}_J - \bar{y}_D) - m_J g
\end{aligned}
\tag{1}
$$

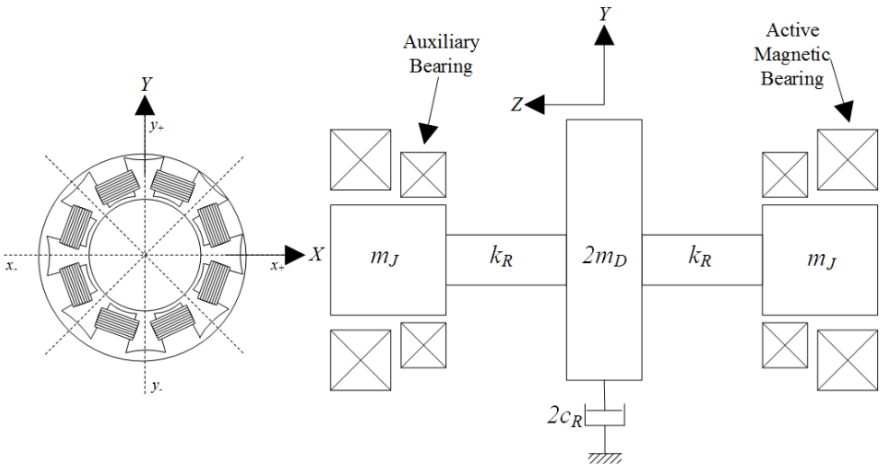

Figure 1. Schematic of a flexible rotor-bearing system.

Eq. (1) can be made non-dimensional by dividing it with $m_D\omega_n^2 g_0$ and introducing the following parameters: $\gamma = \frac{m_J}{m_D}$, $\zeta = \frac{c_R}{2m_D\omega_r}$, $W = \frac{g}{\omega_r^2 g_0}$, $U = \frac{u}{g_0}$, $\Omega = \frac{\omega}{\omega_n}$ and $\tau = \omega_n t$. The linear natural frequency of the magnetic bearing system is denoted by ω_n, and the bearing's nominal air gap is denoted by g_0 g_0. The ratio of the journal mass m_J to half-mass of the disc at the rotor mid-span m_D is denoted by γ, the mass ratio. Half the viscous damping ratio acting at the rotor mid-span is denoted by ζ. W denotes the gravity parameter, and the pin-pin natural frequency of the flexible rotor, ω_r, is

given by $\sqrt{\frac{k_R}{m_D}}$. The ratio of the linear natural frequency of the magnetic bearing system ω_n to the pin-pin natural frequency of the flexible rotor ω_r is denoted as the frequency ratio, $\frac{\omega_n}{\omega_r}$. The ratio of the rotor operating speed ω to the linear natural frequency of the magnetic bearing system ω_n is denoted as the speed parameter, Ω. The non-dimensional rotor imbalance is denoted as unbalance parameter, U, and the non-dimensional time is denoted by τ. The magnetic bearing's nominal air gap is used to transform the displacement, velocity and acceleration of the disk and journal in the X and Y-directions into non-dimensional form. The non-dimensional governing equations for the rotor-bearing system are presented in Eq. (2). The first and second derivatives of the variables with respect to τ are denoted as superscripts ($'$) and ($''$).

$$\begin{aligned}
x_D'' &= -2\zeta\frac{\omega_r}{\omega_n}x_D' - \left(\frac{\omega_r}{\omega_n}\right)^2\left(x_D - x_J\right) + U\Omega^2\cos\Omega\tau \\
y_D'' &= -2\zeta\frac{\omega_r}{\omega_n}y_D' - \left(\frac{\omega_r}{\omega_n}\right)^2\left(y_D - y_J\right) - \left(\frac{\omega_r}{\omega_n}\right)^2 W + U\Omega^2\sin\Omega\tau \\
x_J'' &= \frac{\overline{F}_X}{m_J\omega_n^2 g_0} + \frac{\overline{F}_{AX}}{m_J\omega_n^2 g_0} - \frac{1}{\gamma}\left(\frac{\omega_r}{\omega_n}\right)^2\left(x_J - x_D\right) \\
y_J'' &= \frac{\overline{F}_Y}{m_J\omega_n^2 g_0} + \frac{\overline{F}_{AY}}{m_J\omega_n^2 g_0} - \frac{1}{\gamma}\left(\frac{\omega_r}{\omega_n}\right)^2\left(y_J - y_D\right) - \left(\frac{\omega_r}{\omega_n}\right)^2 W
\end{aligned} \tag{2}$$

The details of the derivation of the magnetic bearing forces have been presented in [8], and the non-dimensional forces are reproduced herein as Eq. (3). The geometric coupling parameter is denoted by α, and the non-dimensional proportional and derivative feedback gains of the magnetic bearing controller are respectively denoted by P and D.

$$\begin{aligned}
F_X &= \frac{\overline{F}_X}{m_J\omega_n^2 g_0} = F_{X+} - F_{X-} + \alpha x_J\left(F_{Y+} + F_{Y-}\right) \\
F_Y &= \frac{\overline{F}_Y}{m_J\omega_n^2 g_0} = F_{Y+} - F_{Y-} + \alpha y_J\left(F_{X+} + F_{X-}\right)
\end{aligned} \tag{3}$$

where

$$F_{X+} = \frac{1}{4(P-1)}\left[\frac{\left(1 - Px_J - Dx_J'\right)^2}{\left(1 - x_J\right)^2}\right] \qquad F_{X-} = \frac{1}{4(P-1)}\left[\frac{\left(1 + Px_J + Dx_J'\right)^2}{\left(1 + x_J\right)^2}\right]$$

$$F_{Y+} = \frac{1}{4(P-1)}\left[\frac{\left(1 - Py_J - Dy_J'\right)^2}{\left(1 - y_J\right)^2}\right] \qquad F_{Y-} = \frac{1}{4(P-1)}\left[\frac{\left(1 + Py_J + Dy_J'\right)^2}{\left(1 + y_J\right)^2}\right]$$

Figure 2 shows the contact forces between the journal and the auxiliary bearing [21]. The normal contact force $\bar{F}_n$ is a function of the auxiliary bearing contact stiffness k and journal penetration depth, e, whilst the friction force $\bar{F}_t$ is a function of the normal force $\bar{F}_n$ and the Coulomb sliding friction coefficient between the rotor and the auxiliary bearing, μ [17-18]. The auxiliary bearing commonly operates at one-half of the magnetic bearing's nominal clearance in practical applications. Eq. (4) represents these contact forces in both the X and Y-directions.

$$\begin{aligned}\overline{F}_{AX} &= -\overline{F}_n \cos\psi + \overline{F}_t \sin\psi \\ \overline{F}_{AY} &= -\overline{F}_n \sin\psi - \overline{F}_t \cos\psi\end{aligned} \tag{4}$$

where

$$\overline{F}_n = \begin{cases} ke & e > 0 \\ 0 & e \le 0 \end{cases}$$

$$\overline{F}_t = \begin{cases} \mu ke & e > 0 \\ 0 & e \le 0 \end{cases}$$

$$e = \sqrt{\bar{x}_J^2 + \bar{y}_J^2} - 0.5 g_0$$

$$\psi = \tan^{-1} \frac{\bar{y}_J}{\bar{x}_J}$$

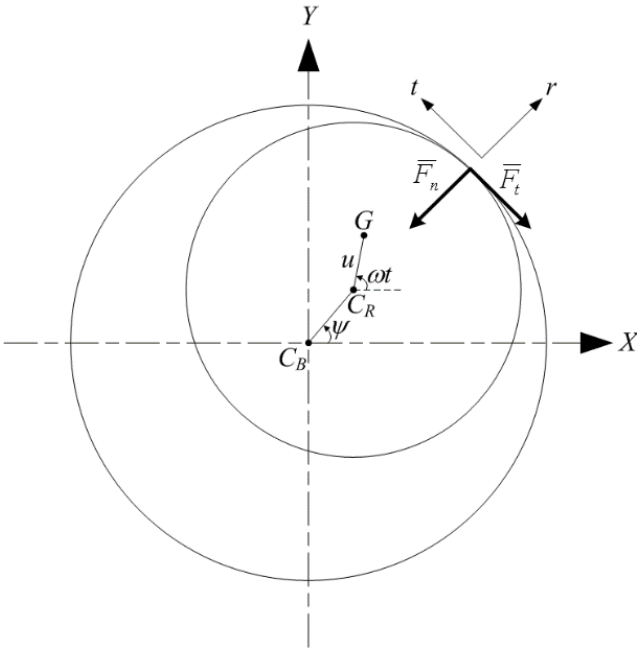

Figure 2. Rotor - auxiliary bearing contact model [21].

The rotor - auxiliary bearing contact forces can be made non-dimensional by dividing Eq. (4) with $m_J \omega_n^2 g_0$. Eq. (5) is obtained by substituting the parameters and variables $K = \frac{k}{m_J \omega_n^2}$, $\varepsilon = \frac{e}{g_0}$, $x_J = \frac{\bar{x}_J}{g_0}$ and $y_J = \frac{\bar{y}_J}{g_0}$ into Eq. (4).

$$\begin{aligned}\frac{\overline{F}_{AX}}{m_J \omega_n^2 g_0} &= -\frac{\overline{F}_n}{m_J \omega_n^2 g_0} \cos\psi + \frac{\overline{F}_t}{m_J \omega_n^2 g_0} \sin\psi \\ \frac{\overline{F}_{AY}}{m_J \omega_n^2 g_0} &= -\frac{\overline{F}_n}{m_J \omega_n^2 g_0} \sin\psi - \frac{\overline{F}_t}{m_J \omega_n^2 g_0} \cos\psi\end{aligned} \tag{5}$$

where

$$\frac{\overline{F}_n}{m_J\omega_n^2 g_0} = \begin{cases} K\varepsilon & \varepsilon > 0 \\ 0 & \varepsilon \le 0 \end{cases}$$

$$\frac{\overline{F}_t}{m_J\omega_n^2 g_0} = \begin{cases} \mu K\varepsilon & \varepsilon > 0 \\ 0 & \varepsilon \le 0 \end{cases}$$

$$\varepsilon = \sqrt{x_J^2 + y_J^2} - 0.5$$

$$\psi = \tan^{-1}\frac{y_J}{x_J}$$

The ratio of the auxiliary bearing contact stiffness to the linear stiffness of the magnetic bearing system is denoted as the stiffness ratio, K. The ratio of the journal penetration depth to the nominal clearance of the magnetic bearing is denoted by ε.

3. Results and Discussion

The governing equations of the rotor-bearing system, Eq. (2), were solved using MATLAB's Runge-Kutta (4,5) algorithm. The following parameters were held constant in the numerical simulation: $W = 0,\ \gamma = 0.2,\ \alpha = 0.24,\ \zeta = 0.001,\ \frac{\omega_n}{\omega_r} = 1.5,\ U = 0.05,\ P = 1.1$ and $D = 0.03$. The speed parameter, Coulomb sliding friction coefficient and stiffness ratio were respectively varied within the following ranges: $0.05 \le \Omega \le 5.0,\ 0 \le \mu \le 0.4$ and $0 \le K \le 5.0$. Figure 3(a) depicts the rotor's response for $\mu = 0$ and $K = 0$ over the range $0.05 \le \Omega \le 5.0$, the case of the omission of the auxiliary bearing in the system model. Figure 3(b), on the other hand, shows the response of the rotor with the auxiliary bearing, $\mu = 0.2$ and $K = 2.5$, over the same speed parameter range. The occurrence of sub-synchronous response of the rotor is observed in Figure 3(a), the case without auxiliary bearing. Specifically period-2, period-4 and period 8 responses were seen in the range $0.23 \le \Omega \le 0.27$, and period-2 response in the range $0.37 \le \Omega \le 0.39$. The rotor response was synchronous for the remaining values of speed parameter considered in his work. For the case of a magnetically supported rigid rotor in auxiliary bearing presented in reference [21], the response was found to be synchronous for the same range of speed parameter, and for the same parameters of the rigid-rotor system. This indicated that the sub-synchronous response seen in Figure 3(a) could be attributed to the flexibility of the rotor, which is represented by the frequency ratio $\frac{\omega_n}{\omega_r} = 1.5$. The incorporation of the auxiliary bearing in the system model resulted in a wider range of speed parameter where sub-synchronous and non-synchronous response of the rotor was observed, Figure 3(b). Specifically such responses were seen in the ranges $0.25 \le \Omega \le 0.93$ and $1.54 \le \Omega \le 2.82$. Synchronous response, on the other hand, was observed in the ranges $0.94 \le \Omega \le 1.53$ and $2.83 \le \Omega \le 5.0$.

Bifurcation diagrams were also generated for the rotor response with variation of the Coulomb sliding friction coefficient, μ, and stiffness ratio, K, and a constant speed parameter $\Omega = 0.75$. These bifurcation diagrams are shown in Figures 4(a) and 4(b) for the rotor response with variation of μ and K, respectively. The bifurcation diagram in Figure 4(a), depicting the response of the rotor with varying Coulomb sliding friction coefficient within the range $0 \le \mu \le 0.4$ and $K = 2.5$, showed that sub-synchronous and non-synchronous vibrations dominated the response. Period-2 response existed for the range $0 \le \mu \le 0.07$ and period-4 in the range $0.071 \le \mu \le 0.113$. Synchronous response of the rotor was not observed within the range $0 \le \mu \le 0.4$ considered in this work. The value of $\frac{\omega_n}{\omega_r} = 1.5$ and $\Omega = 0.75$ used in the simulation yields the rotor's operating speed ω which is equals to $1.125\omega_r$, indicating that the rotor operation was within the vicinity of the rigid bearing critical of the system. Within such region of operation and for $K = 2.5$, the results from the numerical simulation indicated that the Coulomb sliding friction coefficient is not an effective parameter to eliminate sub-

synchronous and non-synchronous response of the rotor during load sharing operation between magnetic and auxiliary bearings.

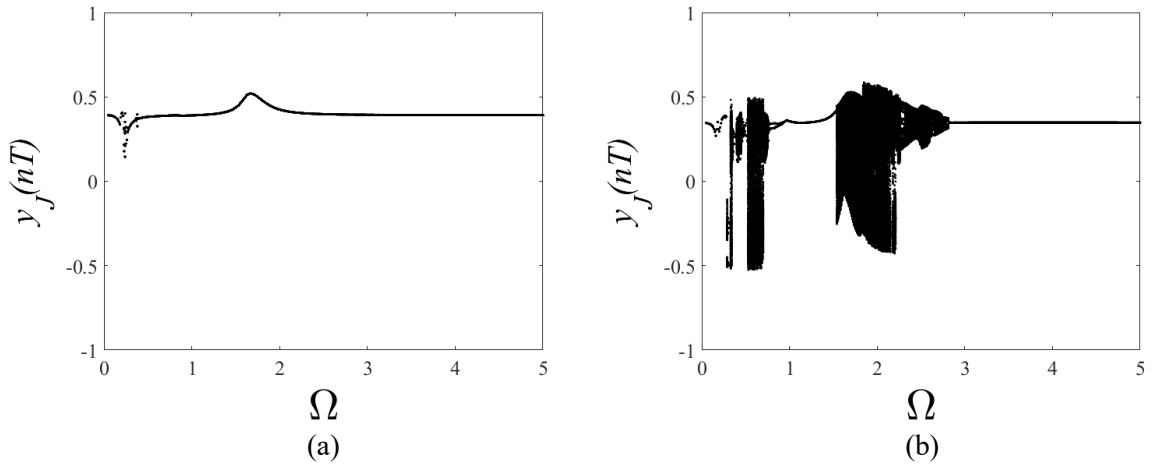

Figure 3. Rotor response for $U = 0.05$, $W = 0$, $\gamma = 0.2$, $\alpha = 0.24$, $\zeta = 0.001$, $\frac{\omega_n}{\omega_r} = 1.5$, $P = 1.1$ and $D = 0.03$: (a) $\mu = 0$ and $K = 0$, (b) $\mu = 0.2$ and $K = 2.5$.

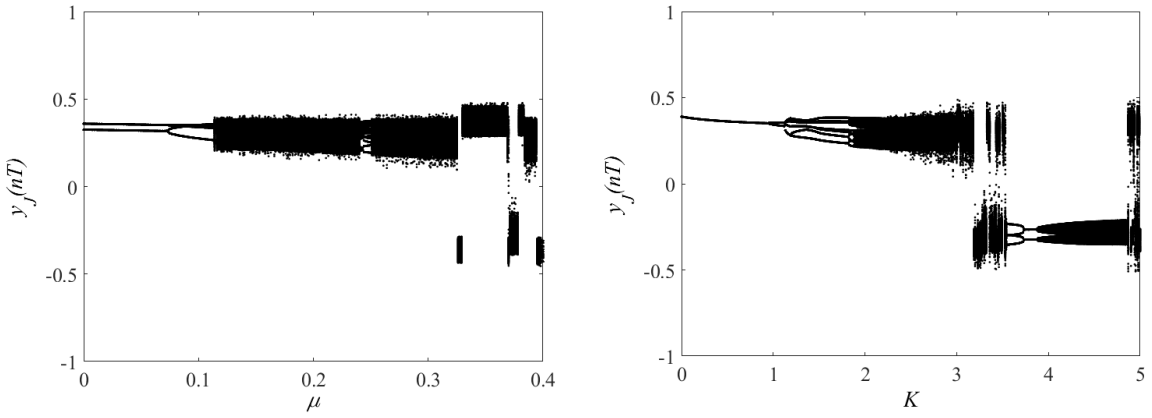

Figure 4. Rotor response for $U = 0.05$, $W = 0$, $\gamma = 0.2$, $\alpha = 0.24$, $\zeta = 0.001$, $\frac{\omega_n}{\omega_r} = 1.5$, $P = 1.1$, $D = 0.03$ and $\Omega = 0.75$: (a) with variation of μ and $K = 2.5$, (b) with variation of K and $\mu = 0.2$.

Figure 4(b) shows the bifurcation diagram for the rotor response with the variation of stiffness ratio in the range $0 \leq K \leq 5.0$ and $\mu = 0.2$. Unlike the case of the rotor response with the variation of the Coulomb sliding friction coefficient shown in Figure 4(a), synchronous response was seen in the rotor response for lower values of the stiffness ratio. Enlargement of Figure 4(b) is shown in Figure 5. It is seen in Figure 5(a) that synchronous response existed for the range $0 \leq K \leq 0.95$. Sub-synchronous response of period-2, period-4, period-8 and period-16 were respectively seen in the ranges $0.96 \leq K \leq 1.12$, $1.13 \leq K \leq 1.19$, $1.20 \leq K \leq 1.81$ and $1.82 \leq K \leq 1.87$. Further increase in the value of the stiffness parameter resulted in non-synchronous response of the rotor, specifically for the range $1.88 \leq K \leq 3.54$, Figure 5. As observed in Figure 5(b), the non-synchronous response of the rotor bifurcated through a reverse period-doubling route into period-4 and period-2 responses for the ranges

$3.55 \leq K \leq 3.73$ and $3.74 \leq K \leq 3.87$, respectively. For the remaining values of the stiffness parameter, $3.88 \leq K \leq 5.0$, non-synchronous vibration dominated the rotor's response.

The existence of synchronous response in the range $0 \leq K \leq 0.95$ indicated that the stiffness ratio is an effective parameter to eliminate sub-synchronous and non-synchronous responses of the rotor. The results concurred with those presented by Inayat-Hussain [21] for the case of a magnetically supported rigid rotor in auxiliary bearings, whereby it was shown that for low value of unbalance parameter, $U = 0.05$, synchronous response existed for smaller values of stiffness parameter. The outcome of the present work and that of Inayat-Hussain [21] on the steady-state response of a rigid and flexible rotor in load sharing operation between magnetic and auxiliary bearings, respectively, is also consistent with the work presented by Kirk [12] on rotor drop onto auxiliary bearings. Similar to the outcome of the work of Kirk [12] on rotor drop analysis, the present work also showed the advantage of soft-mounted auxiliary bearing, namely those with low values of stiffness ratio, for the suppression on sub-synchronous and non-synchronous responses of rotors in load sharing operation between magnetic and auxiliary bearings.

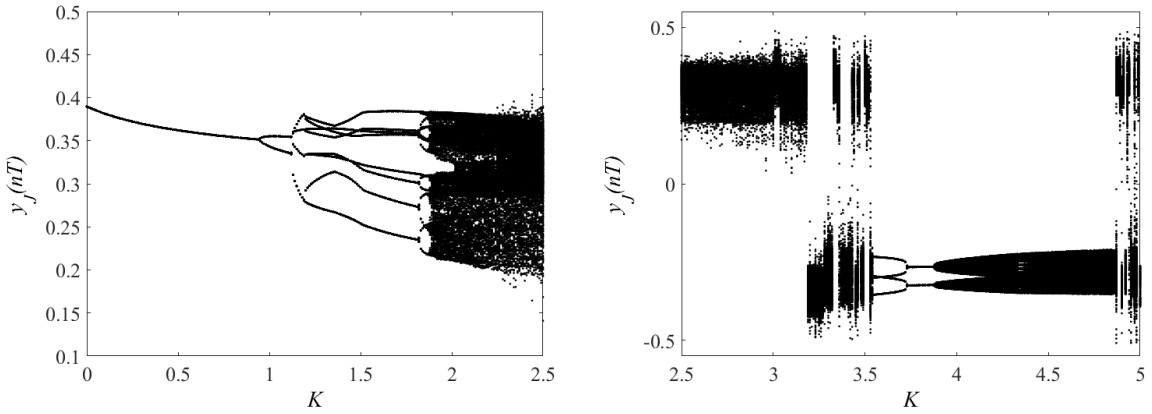

(a) (b)

Figure 5. Enlargement of Figure 3(b) for: (a) $0 \leq K \leq 2.5$, (b) $2.5 \leq K \leq 5.0$.

Sub-synchronous and non-synchronous vibrations are not desirable in the rotors' response as they introduce stress reversals in the rotors and associated structures. Such stresses, if allowed to occur for a long period of time, may cause fatigue failure to the rotors and associated structures. As seen in Figure 5, synchronous response of the rotor undergoes a sequence of period-doubling bifurcation, culminating in non-synchronous response. Figures 6 and 7 show the rotor response for $K = 1.75$ and $K = 2.75$, respectively. As is evident from the Poincaré map and power spectrum plot in these figures, period-16 response is seen for $K = 1.75$, and the non-synchronous response observed for $K = 2.75$ is chaotic vibration. The chaotic response of the rotor for $K = 2.75$ is clearly evidenced by the strange attractor in the Poincaré map and the existence of broadband frequency in the power spectrum plot of Figures 7(b) and 7(c), respectively. The bifurcations of the rotor response from period-1 to period-2, period-4, period-8 and period-16 before the occurrence of chaotic vibration, shown in Figure 4, indicated that the route to chaos was via the period-doubling cascade.

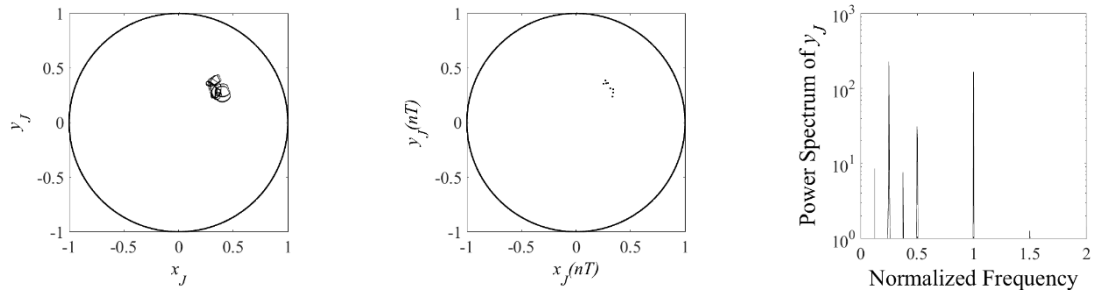

(a) (b) (c)

Figure 6. Rotor response for $U = 0.05$, $W = 0$, $\gamma = 0.2$, $\alpha = 0.24$, $\zeta = 0.001$, $\frac{\omega_n}{\omega_r} = 1.5$, $P = 1.1$, $D = 0.03$, $\Omega = 0.75$, $\mu = 0.2$ and $K = 1.75$: (a) orbit, (b) Poincaré map, (c) power spectrum.

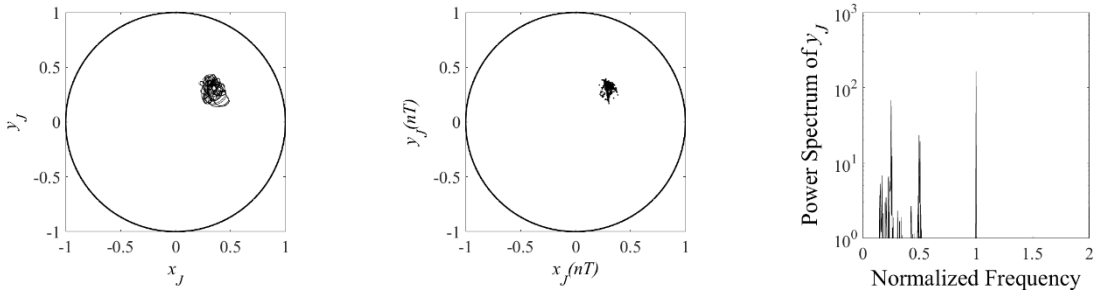

(a) (b) (c)

Figure 7. Rotor response for $U = 0.05$, $W = 0$, $\gamma = 0.2$, $\alpha = 0.24$, $\zeta = 0.001$, $\frac{\omega_n}{\omega_r} = 1.5$, $P = 1.1$, $D = 0.03$, $\Omega = 0.75$, $\mu = 0.2$ and $K = 2.75$: (a) orbit, (b) Poincaré map, (c) power spectrum.

4. Conclusions

The response of a magnetically flexible rotor in auxiliary bearing was investigated via numerical simulation in this work. The work particularly focused on the effect of shaft flexibility in the response of the flexible rotor in load sharing operation between magnetic and auxiliary bearings. For the range of system parameters considered in this work, the numerical results showed that the auxiliary bearing contact stiffness, represented by stiffness ratio, K, was more effective as compared to the Coulomb sliding friction coefficient, μ, for suppressing sub-synchronous and non-synchronous vibrations in the rotor's response. The results further showed the existence of sub-synchronous vibrations of period-2, period-4, period-8 and period-16 in the rotor's response. The non-synchronous response observed were chaotic vibration, and the route to chaos was found to be due to period-doubling cascade in the rotor response when the stiffness parameter was varied for the range $0 \leq K \leq 5.0$. Sub-synchronous and non-synchronous vibrations are to be prevented in the rotating machinery operation as they produce stress reversals, which may in turn cause failure of the rotor and associated machine components due to fatigue.

Acknowledgements

The author gratefully acknowledges the financial support provided by Universiti Tenaga Nasional through the iRMC Pocket Grant (RJO10436494/POCKET/2019003).

References

[1] Chinta M, Palazzolo A B and Kascak A 1996 Quasiperiodic vibration of a rotor in a magnetic bearing with geometric coupling *Proc. of the 5th Int. Symp. on Magnetic Bearings, August 28-30, 1996, Kanazawa, Japan* p. 147-52.

[2] Chinta M and Palazzolo A B 1998 Stability and bifurcation of rotor motion in a magnetic bearing *J Sound Vib* **215** 793-803.
[3] Ji J C, Hansen C H and Zander A C 2008 Nonlinear dynamics of magnetic bearing systems *J Intell Mater Syst Struct* **19** 1471-91.
[4] Hebbale K V and Taylor D L 1986 Nonlinear dynamics of attractive magnetic bearings *Proc. of the Workshop on Rotordynamic Instability Problems in High-Performance Turbomachinery, June 2–4, 1986, Texas A&M University, College Station, Texas, USA* p. 397–418.
[5] Mohamed A M and Emad F P 1993 Nonlinear oscillations in magnetic bearing systems *IEEE Trans Autom Control* **38** 1242-5.
[6] Virgin L N, Walsh T F and Knight J D 1995 Nonlinear behavior of a magnetic bearing system *ASME J Eng Gas Turb Power* **117** 582-8.
[7] Steinschaden N and Springer H 1999 Some nonlinear effects of magnetic bearings *Proc. of DETC99, 17th Biennial ASME Vibrations Conference, September 12-15, 1999, Las Vegas, Nevada, USA* p. 1-7.
[8] Inayat-Hussain J I 2007 Chaos via torus breakdown in the vibration response of a rigid rotor supported by active magnetic bearings *Chaos Solitons Fracts* **31** 912-27.
[9] Inayat-Hussain J I 2010 Nonlinear dynamics of a statically misaligned flexible rotor in active magnetic bearings *Commun Nonlinear Sci Numer Simlat* **15** 764-77.
[10] Fumagalli M and Schweitzer G 1996 Motion of a rotor in retainer bearings *Proc. of the 5th Int. Symp. on Magnetic Bearings, August 28-30, 1996, Kanazawa, Japan* p. 509-514.
[11] Ishii T and Kirk R G 1996 Transient response technique applied to active magnetic bearing machinery during rotor drop *ASME J Vib Acoust* **118** 154-63.
[12] Kirk R G 1999 Evaluation of AMB turbomachinery auxiliary bearings *ASME J Vib Acoust* **121** 156-61.
[13] Karkkainen A, Sopanen J and Mikkola A 2007 Dynamic simulation of a flexible rotor during drop on retainer bearings *J Sound Vib* **306** 601-17.
[14] Zeng S 2003 Modelling and experimental study of the transient response of an active magnetic bearing rotor during rotor drop on back-up bearings *IMechE J Sys Cont Eng* **217** 505-17.
[15] Lawen, Jr. J L and Flowers G T 1997 Synchronous dynamics of a coupled shaft/bearing/housing system with auxiliary support from a clearance bearing: analysis and experiment *ASME J Eng Gas Turb Power* **119** 430-5.
[16] Wang X and Noah S 1998 Nonlinear dynamics of a magnetically supported rotor on safety auxiliary bearings *ASME J Vib Acoust* **120** 596-606.
[17] Xie H, Flowers G T, Feng L and Lawrence C 1999 Steady-state dynamic behavior of a flexible rotor with auxiliary support from a clearance bearing *ASME J Vib Acoust* **121** 78-83.
[18] Jang M J and Chen C K 2001 Bifurcation analysis in flexible rotor supported by active magnetic bearings *Int J Bifurcat Chaos* **11** 2163-78.
[19] Zeng S 2002 Motion of AMB rotor in backup bearings *ASME J Vib Acoust* **124** 460-64.
[20] Inayat-Hussain J I 2011 Bifurcations in the response of a rigid rotor supported by load sharing between magnetic and auxiliary bearings *Meccanica* **46** 1341-51.
[21] Inayat-Hussain J I 2010 Nonlinear dynamics of a magnetically supported rigid rotor in auxiliary bearings *Mech Mach Theory* **45** 1651-67.